Progress In Electromagnetics Research C, Vol. 49, 11–17, 2014

Dual-Band Circularly Polarized Antenna with Differential Feeding

Jianjun Wu*, Yingzeng Yin, Zedong Wang, and Ruina Lian

Abstract—A dual-band circularly polarized antenna is presented in this paper. A rectangular patch antenna with gap-feeding structure is firstly designed, and 3-dB axial-ratio bandwidth from 2.35 to 2.48 GHz is obtained. A parasitic square ring is placed on the rear of the rectangular patch as a band-notch unit operating around 2.4 GHz. Then an original wide circularly polarized band is split into two bands from 2.25 to 2.31 GHz and from 2.46 to 2.53 GHz. By adopting differential feeding, symmetrical patterns are achieved. Measurement results show that two 3-dB axial-ratio bands of 2.6% (2.25–2.31 GHz) and 2.0% (2.51–2.56 GHz) are obtained with a small frequency ratio of 1.11.

1. INTRODUCTION

Circularly polarized (CP) antennas are more and more popular in wireless communication systems because they are independent of the transmitting and receiving orientations [1–4]. Due to various spectrum requirements, dual-band CP operations are also required, and various types of antenna structures with dual-band CP properties have been reported [5–11]. Techniques such as stacked-patch configurations [5, 6] and employing different resonant elements on a single layer [7, 8] are often adopted to realize dual bands. But achieving a small frequency ratio of the two bands and wide axial-ratio (AR) bandwidths with a simple structure is still a challenge in dual-band CP antenna designs. In [9], a dual-band CP antenna with unequal T-slotted slits in truncated corners obtains a small frequency ratio of 1.07. Two annular rings are placed on opposite sides of a substrate to excite dual-band waves in [10], and the frequency ratio can be varied from 1.28 to 1.83 by adjusting the radius of the patch. In [11], dual-band CP operation with frequency ratio of 1.18 is achieved by adopting a circular patch below a rotated rectangular patch. In this design, the lower frequency is mainly dictated by the rectangular patch and the higher frequency mainly dictated by the circular patch.

Moreover, there is increasing interest in antennas with differential signal operation recently [12–16]. This is because the differential signal operation is more suitable for radio frequency integrated circuits [12]. The receiver noise performance and transmitter power efficiency can be greatly improved by adopting differential signals [13]. In addition, single-ended antennas and baluns which convert differential signals to single-ended signals can be replaced merely by differentially-driven antennas. Thus loss on chip baluns can be decreased, and better polarization purity is observed [14, 15]. For example, a differential dual-band antenna is introduced in [14], and dual bands are achieved by multilayer structure. Another differentially-driven dual-polarized antenna is proposed in [15], and its cross-polarization level is very low due to the differentially-driven scheme. But CP antennas with differential operation have rarely been mentioned in current literatures. A differentially-fed antenna in [16] focuses on omnidirectional circular polarization. Another broadband CP patch antenna, differentially-fed by a pair of folded plate, is presented in [17], and the radiation patterns of both E- and H-planes are symmetrical. And the differential feeding is imitated by using a Wilkinson balun with microstrip metamaterial lines in [18].

In this paper, a dual-band CP antenna with a small frequency ratio of 1.11 is presented and discussed. By placing a square ring on the back of a rectangular patch, the original single CP band is

Received 6 March 2014, Accepted 25 March 2014, Scheduled 1 April 2014

* Corresponding author: Jianjun Wu (jun542391752@126.com).

The authors are with the Science and Technology on Antenna and Microwave Laboratory, Xidian University, Xi'an, Shaanxi 710071, China.

split into two bands. Good radiation characteristics are obtained by additionally adopting differential feeding. Details of the antenna design are introduced and the measured results also presented.

2. ANTENNA DESIGN

The geometry of the proposed dual-band CP antenna is shown in Figure 1. A rectangular patch with size $L \times W$ is printed on a square FR4 substrate with length of S, thickness of 1 mm and relative permittivity of 4.4. And the substrate is placed above a metal ground with a height of H. Another square ring with length of L_s and width of W_s is printed on the bottom layer of the substrate with the same center as rectangular patch. Two symmetric small feeding patches of $a \times b$ are located on the same layer of the rectangular patch with distances of g_1 and g_2 from the edges of the main radiating patch. The two feeding structures are connected to SMA ports with long probes. Figure 2 depicts the design evolution process of the proposed antenna. Antenna 1 is a rectangular patch with single gap feeding, and a square ring is added on the back to form Antenna 2. Antenna 3 is differentially fed, and the same square ring is adopted to configure the final Antenna 4. All the optimal antenna parameters obtained by Ansoft HFSS 13 software is tabulated in Table 1. And the details of antenna design and operating mechanisms are discussed in the following section.

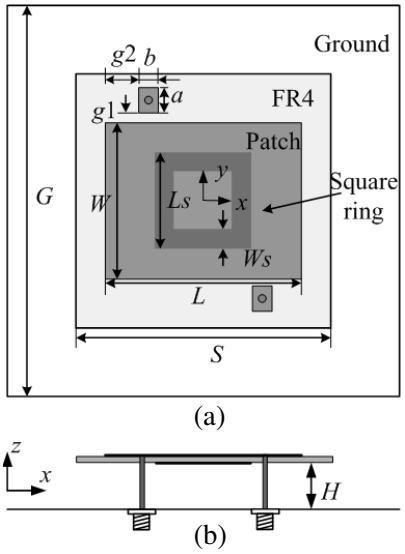

Figure 1. Geometry of the proposed antenna: (a) top view and (b) side view.

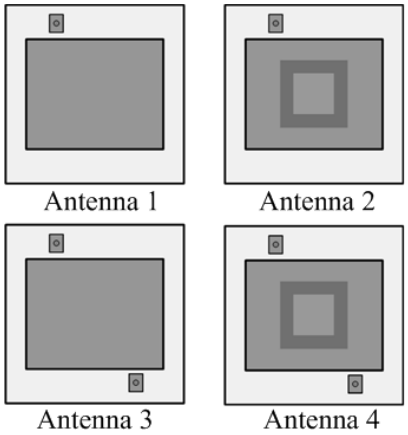

Figure 2. Antenna design evolution process.

Table 1. Optimal dimensions of the four CP antennas (Unit: mm).

Parameters	L	W	L_s	W_s	H	G	S	a	b	g_1	g_2
Antenna 1	45	35	—	—	10	120	70	7	7	1.2	5
Antenna 2	45	35	22.7	5	10	120	70	7	7	1.2	5
Antenna 3	45	32	—	—	10	120	70	8	6	3	9
Antenna 4	45	32	22.7	5	10	120	70	8	6	3	9

2.1. Design of CP Antennas with Gap-Feeding

Rectangular patch in Antenna 1 has unequal lengths, and CP waves are yielded when it is fed along the diagonal. The patch is about $0.08\lambda_0$ (λ_0 is the corresponding wavelength of 2.4 GHz) above the ground,

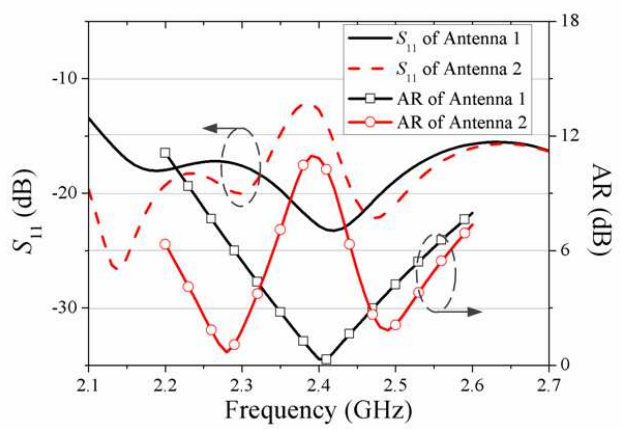

Figure 3. S_{11}s and ARs of antennas with air-gap feeding.

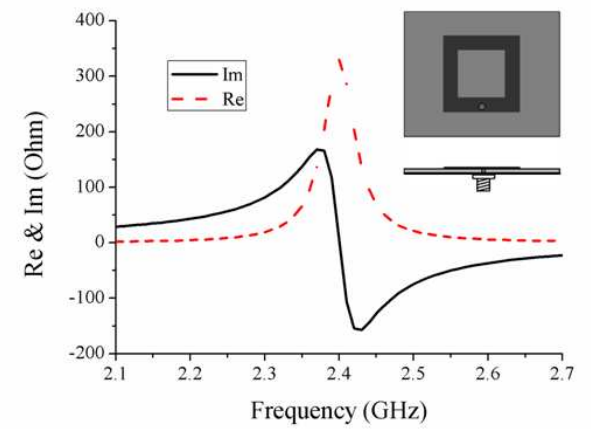

Figure 4. Impedance of ring patch.

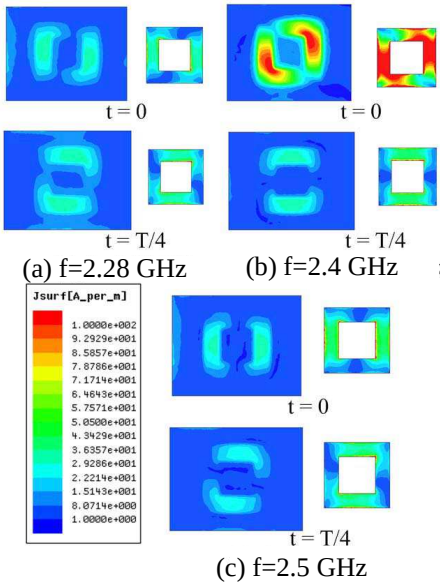

Figure 5. Current distributions on rectangular patch and parasitic ring at different frequencies.

and the long probe introduces large inductance. To achieve good impedance matching, air-gap feeding structure in [3, 4] is adopted in our design. Inductance of the long probe can be compensated by the capacitance between the patch and the feeding point. A square ring is added to the rear of the patch to obtain dual-band operation in Antenna 2. Figure 3 shows the simulated S_{11}s and ARs of patches without parasitic ring and with ring. It can be seen that the original rectangular patch has a wide 3-dB AR bandwidth of 5.4% (2.34–2.47 GHz) and perfect impedance due to air-gap feeding. After inserting square ring, the origin AR band is split into two bands of 2.24–2.31 GHz and 2.47–2.52 GHz. Both S_{11} and AR become worse at center frequency 2.4 GHz.

To understand the dual-band mechanism of Antenna 2, the effects of square ring are studied. The impedance of the ring is simulated on the same substrate with the patch as ground, and the results in Figure 4 show that the ring has a resonant frequency around 2.4 GHz. Additionally, the ring has a perimeter of 70.8 mm ($(L_s - W_s) \times 4$) which is nearly equal to one λ (corresponding wavelength of 2.4 GHz in consideration of the effect of substrate). Current distributions on rectangular patch and parasitic ring in Antenna 2 at different frequencies are depicted in Figure 5. It is noteworthy that the ring has currents with the opposite direction of that on the upper patch but larger amplitude. When

antenna operates at 2.4 GHz, current distributions are unequal within a quarter cycle, and the square ring is in resonant mode. Consequently, band-notched effect around 2.4 GHz is realized due to the added ring. Both the currents on ring and upper patch rotate in anticlockwise direction with uniform amplitude at 2.28 GHz and 2.5 GHz. While more currents are gathered along the edges of rectangular patch in the lower band than higher band. We can conclude that the lower band is mainly determined by the rectangular patch, and higher band is mainly influenced by square ring. The square ring plays not only a band-notched role at 2.4 GHz, but also an important CP role in lower and higher bands.

2.2. Design of Antennas with Differential Feeding

The differential feeding ports in Antenna 3 are symmetrical with respect to the patch center. Both probes are separated from the rectangle corner to comply air-gap feeding. CP performance of the same polarization can be achieved when one probe is located at upper-left corner or lower-right corner singly. While in differential feeding scheme, the two probes are fed with the same amplitude but out of phase. The currents on the two probes flow in opposite directions, and consequently their leakage radiation is canceled. As a result, the currents distribution on the patch is symmetrical, and radiation performance is enhanced. We adopt the differential reflection coefficient S_{dd} of differential ports defined as [15],

$$S_{dd} = 1/2(S_{11} - S_{12} - S_{21} + S_{22}) \tag{1}$$

From the radiation patterns of Antenna 1 and Antenna 3 shown in Figure 6, we can see the advantage of differential feeding on radiation characteristics. The original single-fed Antenna 1 has asymmetric radiation patterns. Cross polarization of left-hand circular polarization (LHCP) is especially more obvious. Thus asymmetric 3-dB AR bandwidth can be seen in the two main planes, and simulated maximum right-hand circular polarization (RHCP) is located at Phi = 242° and Theta = 5° due to unbalanced feeding. For Antenna 3 with differential feeding, symmetric radiation patterns are obtained, and the maximum RHCP is along $+z$-axis. Square ring with the same dimension as that in Antenna 2 is also added in Antenna 4. From the S_{dd}s and ARs shown in Figure 7, we can see that two CP bands of 2.25–2.32 GHz and 2.47–2.54 GHz are split from the original band of 2.35–2.48 GHz. Moreover, S_{dd} at 2.4 GHz in Antenna 4 is above −10 dB, and bad impedance matching is achieved at the useless frequency.

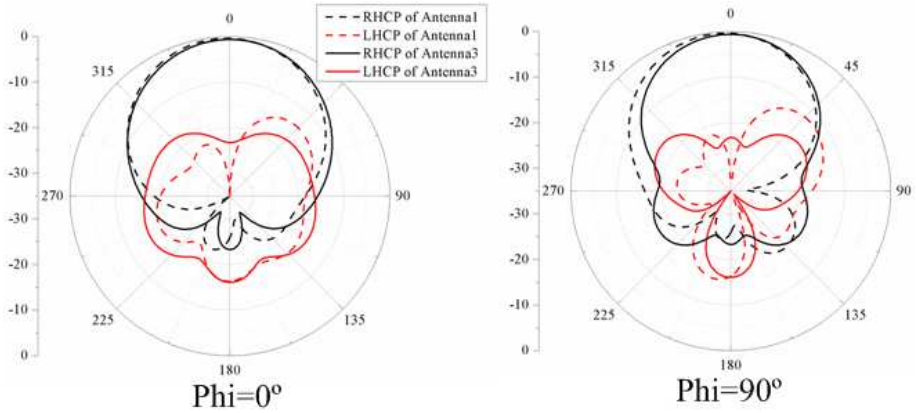

Figure 6. Radiation patterns of antennas with single feeding and differential feeding.

3. EXPERIMENTAL RESULTS

To validate the design strategy, a prototype of the proposed differentially-fed antenna was built, as shown in Figure 8. The differential signal is achieved by using a wideband power divider with metamaterial lines in [18]. The balun comprises a Wilkinson divider, followed by a +90° negative-refractive-index metamaterial (MM) phase-shifting line along one branch, and a −90° phase-shifting line along the other

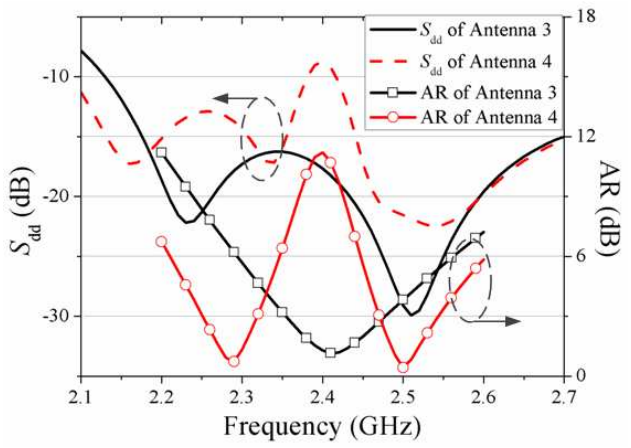

Figure 7. S_{dd}s and ARs of antennas with differential feeding.

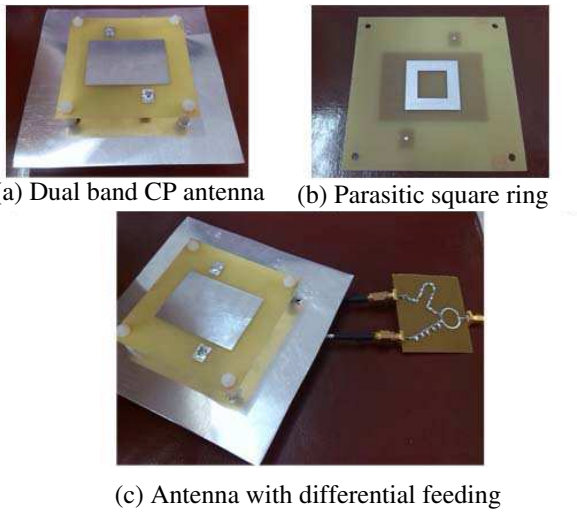

Figure 8. Photos of the fabricated antenna.

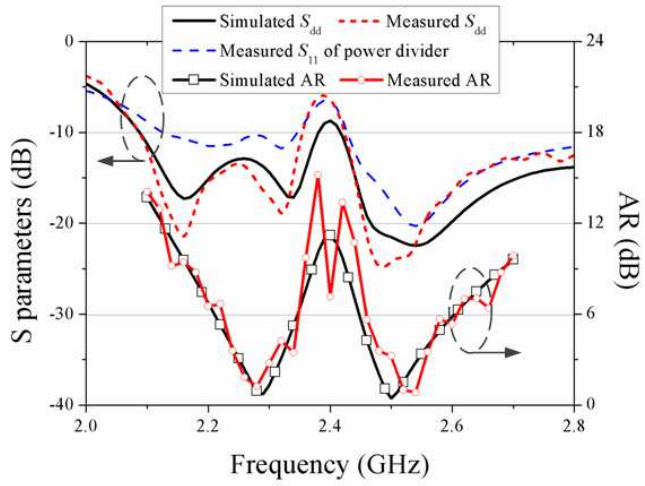

Figure 9. Simulated and measured results of proposed antenna.

branch. Utilizing MM lines for both the $+90°$ and $-90°$ branches maintains a differential output signal over a wider bandwidth than conventional 180° phase shifter using transmission lines.

S_{dd} was measured using a vector network analyzer, and radiation properties were measured by a Satimo StarLab system. Figure 9 shows the measured and simulated S parameters and AR curves of the proposed antenna. Measured 3-dB axial-ratio bands of 2.6% (2.25–2.31 GHz) and 2.0% (2.51–2.56 GHz) are obtained with good impedance matching in both bands. And large return loss and AR value can be seen at center frequency 2.4 GHz. There exists a good consistency between measured and simulated results. The S_{11} parameter of the power divider connected with antenna is also given which is a little higher than S_{dd} in low band. Radiation patterns at 2.28 GHz and 2.53 GHz are shown in Figure 10. Stable radiation patterns of RHCP are yielded along $+z$-axis. The 3-dB AR beamwidths are 67° for xoz-plane and 60° for yoz-plane at 2.28 GHz and 60° and 55° at 2.53 GHz. Figure 11 shows the measured gain and radiation efficiency of the antenna. The gain of RHCP along $+z$-axis is around 8.2 dB in lower band and 8.8 dB in higher band, and the efficiency is about 90% within the two effective bandwidths, which is filled with gray color in Figure 11. While at 2.4 GHz, the gain is 4.5 dB, and efficiency is as low as 25%, which show that the antenna has a poor performance at 2.4 GHz.

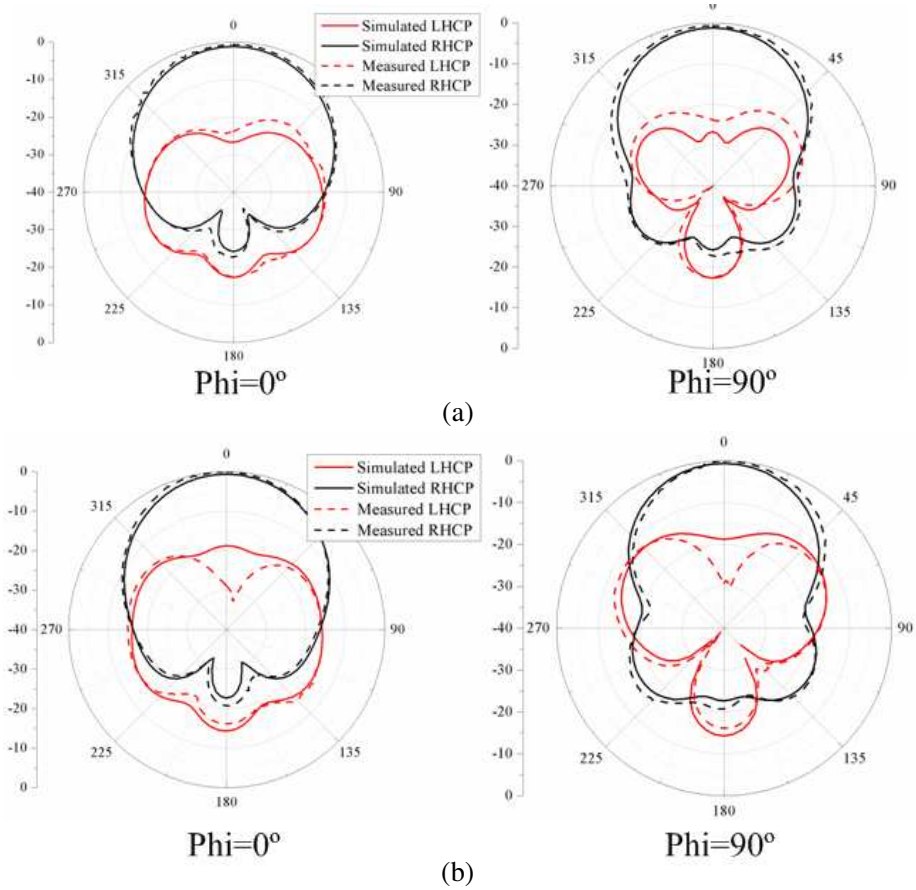

Figure 10. Simulated and measured radiation patterns at (a) 2.28 GHz and (b) 2.53 GHz.

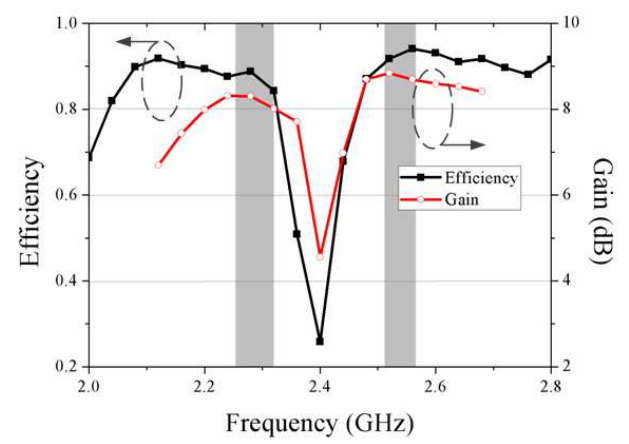

Figure 11. Measured gain and efficiency.

4. CONCLUSION

This paper describes a differentially-fed antenna with dual-band circular polarization. By arranging a square ring on the back of a rectangular patch, dual-band CP operations with a small frequency ratio of 1.11 are achieved. Compared to the differential-fed antenna in [17], the proposed antenna has a simple but effective air-gap feeding structure. Furthermore, the antenna shows good symmetry radiation patterns with RHCP in $+z$ space within the two operating bands.

REFERENCES

1. Zhao, Y., Z. Zhang, K. Wei, and Z. Feng, "A dual circularly polarized waveguide antenna with bidirectional radiations of the same sense," *IEEE Transactions on Antennas and Propagation*, Vol. 62, No. 1, 480–484, 2014.
2. He, Y., W. He, and H. Wong, "A wideband circularly polarized cross-dipole antenna," *IEEE Antennas Wireless Propagation Letters*, Vol. 13 , 67–70, 2014.
3. Kim, S. M. and W. G. Yang, "Single feed wideband circular polarised patch antenna," *Electronics Letters*, Vol. 43, No. 13, 703–704, 2007.
4. Deng, J., L. Guo, T. Fan, Z. Wu, Y. Hu, and J. Yang, "Wideband circularly polarized suspended patch antenna with indented edge and gap-coupled feed," *Progress In Electromagnetics Research*, Vol. 135, 151–159, 2013.
5. Nayeri, P., K.-F. Lee, A. Z. Elsherbeni, and F. Yang, "Dual-band circularly polarized antennas using stacked patches with asymmetric U-slots," *IEEE Antennas Wireless Propagation Letters*, Vol. 10, 492–495, 2011.
6. Ma, S.-L. and J.-S. Row, "Design of single-feed dual-frequency patch antenna for GPS and WLAN applications," *IEEE Transactions on Antennas and Propagation*, Vol. 59, No. 9, 3433–3436, 2011.
7. Bao, X. L. and M. J. Ammann, "Dual-frequency circularly-polarized patch antenna with compact size and small frequency ratio," *IEEE Transactions on Antennas and Propagation*, Vol. 55, No. 7, 2104–2107, 2007.
8. Hsieh, W.-T., T.-H. Chang, and J.-F. Kiang, "Dual-band circularly polarized cavity-backed annular slot antenna for GPS receiver," *IEEE Transactions on Antennas and Propagation*, Vol. 60, No. 4, 2076–2080, 2012.
9. Gaffar, M., M. A. Zaman, and S. M. Choudhury, and M. A. Matin, "Design and optimization of a novel dual-band circularly polarized microstrip antenna," *IET Microwaves, Antennas and Propagation*, Vol. 5, No. 14, 1670–1674, 2011.
10. Sun, X., Z. Zhang, and Z. Feng, "Dual-band circularly polarized stacked annular-ring patch antenna for GPS application," *IEEE Antennas Wireless Propagation Letters*, Vol. 10, 49–52, 2011.
11. Deng, C., Y. Li, Z. Zhang, G. Pan, and Z. Feng, "Dual-band circularly polarized rotated patch antenna with a parasitic circular patch loading," *IEEE Antennas Wireless Propagation Letters*, Vol. 12, 492–495, 2013.
12. Xue, Q., X. Y. Zhang, and C.-H. K. Chin, "A novel differential-fed patch antenna," *IEEE Antennas Wireless Propagation Letters*, Vol. 5, 471–474, 2006.
13. Zhang, Y. P., "Design and experiment on differentially-driven microstrip antennas," *IEEE Transactions on Antennas and Propagation*, Vol. 55, No. 10, 2701–2708, 2007.
14. Wu, H., J. Zhang, L. Yan, L. Han, R. Yang, and W. Zhang, "Differential dual-band antenna-in-package with T-shaped slots," *IEEE Antennas Wireless Propagation Letters*, Vol. 11, 1446–1449, 2012.
15. Xue, Q., S. W. Liao, and J. H. Xu, "A differentially-driven dual-polarized magneto-electric dipole antenna," *IEEE Transactions on Antennas and Propagation*, Vol. 61, No. 1, 425–430, 2013.
16. Bao, X. L. and M. J. Ammann, "Differentially-fed microstrip patch antenna for omni-directional GPS applications," *Loughborough Antennas and Propagation Conference*, 18–21, 2013.
17. Zhang, X. and M. Y. Xia, "A broadband circular polarization patch antenna with differential-feeding," *International Conference on Microwave Technology and Computational Electromagnetics*, 109–112, 2009.
18. Antoniades, M. A. and G. Y. Eleftheriades, "A broadband Wilkinson balun using microstrip metamaterial lines," *IEEE Antennas Wireless Propagation Letters*, Vol. 4 , 209–212, 2005.